INCORPORATING VERTICAL VELOCITY AND BALLOON TRAJECTORY DATA INTO RADIOSONDE GRAVITY WAVE ANALYSIS: OROGRAPHIC SOURCES IN NEW ZEALAND DURING THE DEEPWAVE CAMPAIGN

Tyler Mixa [1,2], Lakshmi Kantha[1], David Fritts[2], Andreas Dörnbrack[3], Sonja Gisinger[3], Johannes Wagner[3]

[1] University of Colorado Boulder, Boulder, CO, USA [2] GATS-inc, Boulder, CO, USA [3] German Aerospace Center (DLR), Germany

ABSTRACT

Conventional analysis of gravity waves from radiosonde data (e.g. Eckermann 1996, Murphy et al. 2014) assumes that the sonde balloon ascent is vertical. It also ignores vertical wind information that can be derived from sonde vertical motion, thus using only temperature and zonal/meridional wind fluctuations to extract wave properties. Sonde-derived profiles have been treated as vertical profiles in applications such as long-term climatology, where the desired background temperature and wind fields exhibit self-similarity over sufficiently large horizontal scales to approximate the measurements as vertical profiles. However, the sonde balloon drifts with the winds, and strong horizontal winds can carry the sonde sufficiently far away from the launch site to cause significant errors in the deduced "vertical" wavelength.

The vertical component of the wind is another metric of gravity wave activity. Wave analysis based on only temperature and horizontal wind fluctuations does not account for this. Some recent studies (e.g. Zhang et al. 2012) have tried to incorporate vertical wind measurements into wave analysis, but the derived wave characteristics may lack dynamical consistency.

We propose an alternative analysis technique that incorporates sonde-derived vertical wind measurements and sonde trajectory data to map regions of significant orographic wave activity. The data were collected during the DEEPWAVE field campaign, where a comprehensive suite of ground-based and airborne sensors were deployed, along with radiosondes, to measure gravity wave propagation up to 100 km altitude over the South Island of New Zealand during the 2014 austral winter. Using the resulting sonde data, we present a preliminary evaluation of orographic wave characteristics incorporating vertical wind and trajectory information, comparing the characteristics to those derived from conventional Stokes parameter analysis.

WAVE EXTRACTION

Gravity wave signatures are identified by fluctuations in the temperature, wind, and ascent rate fields measured by the sonde. Using Reynolds decomposition, these quantities are split into mean (background) and fluctuating components:

$$\{T, u, v, w\} = \overline{\{T, u, v, w\}} + \{T, u, v, w\}'$$

Because the time-averaged background profiles only vary over large spatial scales, spatial filtering can be used to identify the fluctuating components. Fluctuations demonstrating sinusoidal tendencies that fall within reasonable range of vertical wavelengths correspond to Gravity Waves.

Temperature and horizontal wind speed are measured directly by the sonde where the balloon acts as a Lagrangian tracer. Vertical wind speed must be inferred from the balloon ascent rate – it cannot be measured directly because vertical position measurements are neither Eulerian nor Lagrangian with respect to the background airflow. However, because $\overline{w} = 0$, small-scale fluctuations in ascent rate correspond to w'.

To distinguish w' due to gravity waves from w' due to turbulent-laminar transitions of boundary layer flow over the surface of the balloon, w' data can only be collected above the altitude for which airflow over the balloon surface will remain laminar, usually near or above the tropopause.

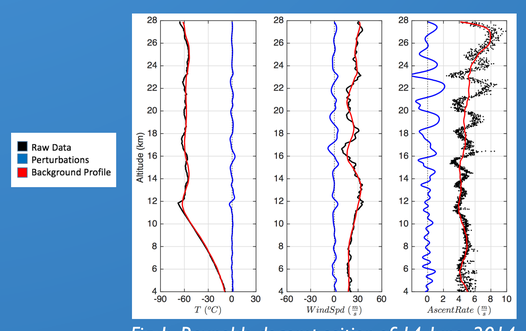

Fig. I: Reynolds decomposition of 14 June, 2014 sounding in Haast, NZ.

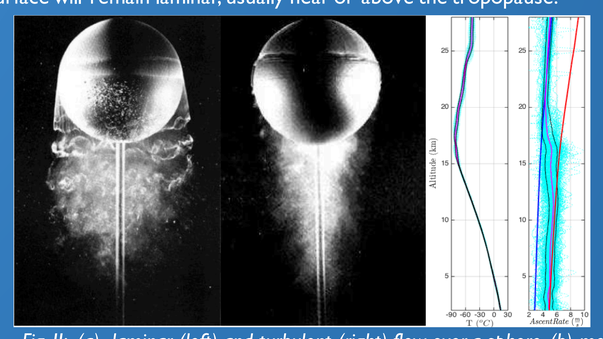

Fig. II: (a) laminar (left) and turbulent (right) flow over a sphere. (b) mean balloon ascent rate (▫) from CPEA II soundings showing transition from turbulent (▫) to laminar (▫) drag regimes near troposphere [Kantha et al. 2015].

UTILITY OF INCORPORATING W' AND SONDE TRAJECTORY INTO WAVE ANALYSIS:

w' sensitivity to higher frequencies allows analysis of broader wave spectrum while providing additional verification of the wave packets with corresponding T' and u' fluctuations. It also allows for the calculation of the intrinsic wave frequency (ω) using kinetic and potential energy as an alternative to determining it from Stokes parameters. This is done by equating the wave frequency obtained from the two expressions

$$\frac{\omega^2}{N^2} = \frac{E_{Kw}}{E_P} \quad and \quad \frac{\omega^2}{f^2} = \frac{E_{Kh}+E_P-E_{Kw}}{E_{Kh}-E_P+E_{Kw}},$$

and solving for E_P, where

$$E_P = \frac{\rho}{2}\left(\frac{g^2}{N^2}\right)\overline{\theta'^2},\ E_{Kh} = \frac{\rho}{2}\left(\overline{u'^2}+\overline{v'^2}\right),\ and \quad E_{Kw} = \frac{\rho}{2}\left(\overline{w'^2}\right).$$

w' information derived from the sonde also allows direct measurement of momentum fluxes. Trajectory data allows the use of radiosonde profiles as a mapping tool, providing a more complete qualitative understanding of gravity wave packets measured by the sonde.

Contextualize wave oscillations with location and altitude

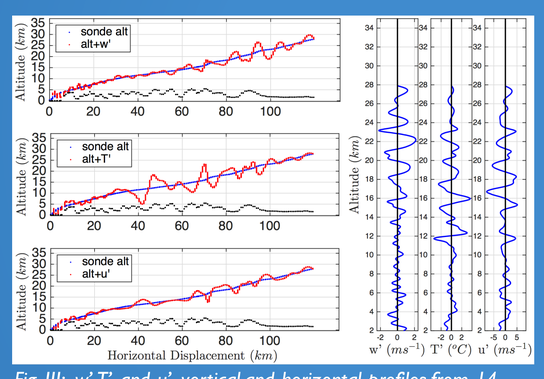

Fig. III: w',T', and u' vertical and horizontal profiles from 14 June, 2014 sounding in Haast, NZ.

Directly measure momentum flux and identify regions of vertical propagation

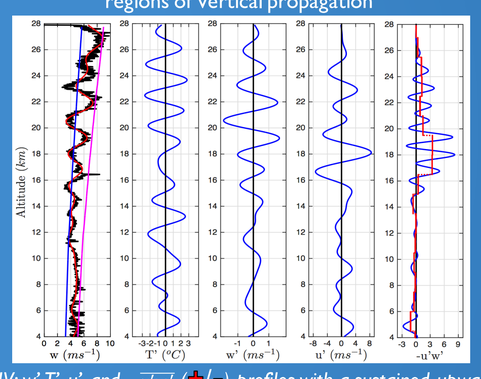

Fig. IV: w',T', u', and $-\overline{u'w'}$ (+/▫) profiles with a sustained upward flux region from 14 June, 2014 sounding in Haast, NZ.

Identify stationary wavefronts over successive soundings

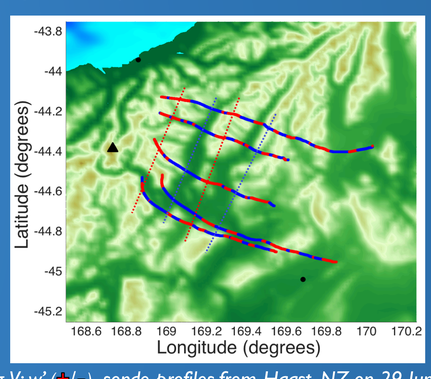

Fig.V: w' (+/▫) sonde profiles from Haast, NZ on 29 June, 2014 showing stationary wavefronts over 16 hours that are consistent with orography.

VALIDATION AND DEEPWAVE COMPARATIVE ANALYSIS

Support for Validity of w' Measurement:

Sample WRF model comparison shows good agreement of wave frequency and wavefront spatial location

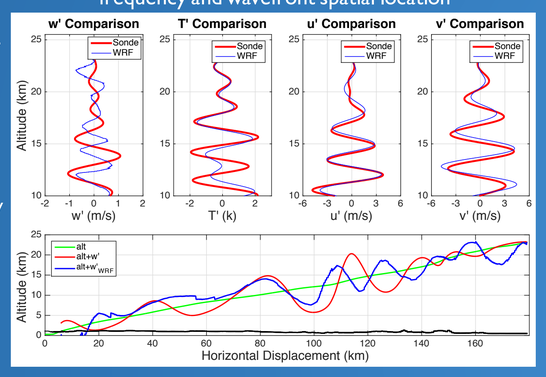

Fig.VI: w',T', u', and v' comparison of sonde- and WRF- derived wave parameters. Data taken from 2014 GW-LCYCLE campaign, provided by Andreas Dörnbrack and Johannes Wagner.

Flux measurements support aircraft observations of wave breaking at flight altitude

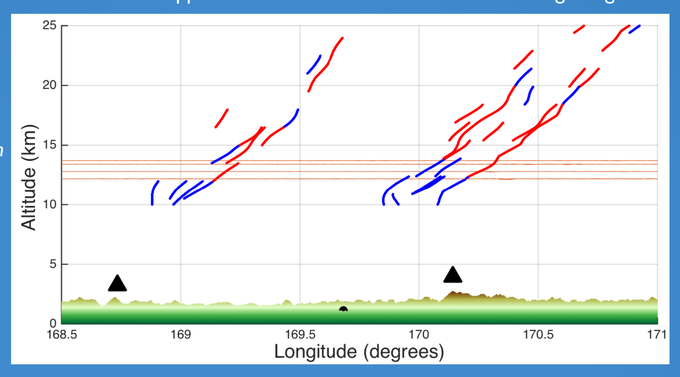

Fig.VII: Aircraft trajectory (▫) and sonde $-\overline{u'w'}$ (+/▫) measurements from Lauder, NZ, and Haast, NZ on 29 June, 2014 showing wave breaking at flight altitude.

w' spectrum peaks at same vertical wavelengths as T' and u', appearing to correspond to the same wave packets

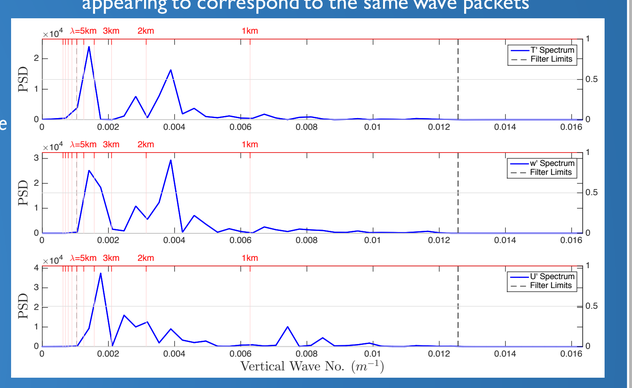

Fig.VIII: T', w', and u' wavenumber spectrum from sample Lauder, NZ sounding on 19 June 2014 showing shared wavenumber peaks.

DEEPWAVE Comparison with Stokes Parameter Analysis

Sounding	λz (km)		ω (1/s)		ω/f		EP (J/kg)			EKh (J/kg)		EKw (J/kg)	EK/EP		
19/6/2014:	Wavelet Analysis	Spatial Filtering	Stokes	EKw,EP,w',T'	Stokes	EKw,EP,w',T'	Stokes(T')	T'	EKh,EKw	Stokes(u',v')	u',v'	w'	EP(Stokes)	EP(T')	EP(EKh,EKw)
5:33 UT	1.50	1.67	4.43E-04	5.22E-03	4.3	54.6	4.571	10.476	2.954	1.363	1.603	1.352	0.298	0.282	1.000
	1.70		3.24E-04		3.1		2.497			4.789			1.918		
	3.30	3.14	2.00E-04	2.25E-03	2.0	23.6	0.872	1.942	1.883	2.094	1.839	0.050	2.403	0.947	1.003
	3.90	3.46	3.68E-04	4.58E-03	3.6	47.9	0.818	1.251	0.324	1.292	0.185	0.140	1.580	0.148	1.000
	5.10	4.48	2.69E-04	1.01E-03	2.6	10.6	1.548	3.914	0.435	4.234	0.416	0.020	2.735	0.106	1.002
		4.79		6.13E-04		6.4		2.211	0.177		0.173	0.004		0.078	1.005
11:31 UT	1.30	1.31	1.06E-03	5.80E-03	10.2	60.9	0.296	4.290	1.900	0.511	1.381	0.525	1.724	0.322	1.003
	1.70	1.66	1.65E-04	7.08E-03	1.6	74.0	2.399	6.670	2.120	1.817	0.888	1.230	0.757	0.133	0.999
14:31 UT	1.20	1.04	2.78E-04	8.13E-03	2.7	85.0	0.251	1.165	1.913	0.295	1.683	0.231	1.174	1.444	1.000
		1.29		7.93E-03		73.7		1.303	1.647		1.398	0.250		1.073	1.000
	2.30	2.06	3.04E-04	6.66E-03	2.9	69.6	3.820	3.984	1.300	1.587	0.801	0.499	0.415	0.201	1.000
	2.80	3.01	3.69E-03	4.19E-03	35.8	43.8	2.129	2.233	1.001	1.030	0.886	0.115	0.484	0.397	1.000
	2.80	3.12	2.09E-04	4.27E-03	2.0	44.6	3.892	2.617	2.092	3.749	1.948	0.145	0.963	0.744	1.001
	5.60	5.52	3.07E-04	8.15E-04	3.0	8.5	1.299	0.088	0.023	0.376	0.023	0.000	0.289	0.258	1.008

Table I: Wave parameters calculated from from soundings in Lauder, NZ on 19 June 2014, using Stokes parameter/wavelet analysis of T'/u'/v', and spatial filtering of T'/u'/v'/w'. Stokes parameter data provided by Sonja Gisinger.

Spatial filtering selects wavelengths with collocated T', u', and w' peaks, and the derived properties are compared to the Stokes-derived parameters of the nearest wavelength packet found by wavelet analysis of u' and v'. Some significant findings include:

- Stokes analysis consistently derives low (near-f) ω. Conversely, ω is an order of magnitude larger for w' calculations than for Stokes parameter analysis based on u' and v', showing that w'-based analysis favors higher frequency (near-N) waves. Near-inertial ω(w') only occur for wave packets having E_{Kw} near zero.
- $E_P(T')$ is significantly larger than $E_P(E_{Kh},E_{Kw})$ and E_P(Stokes), indicating that T' fluctuations may overestimate E_P.
- $E_K/E_P(Stokes) \approx 2$, indicating inertial-internal waves, but the data in several wave packets with E_K/E_P(Stokes) << 1 may be erroneous and misleading. $E_K/E_P(T') < 1$ supports the argument that $E_P(T')$ is overestimated, whereas $E_K/E_P(E_{Kh},E_{Kw})$ is consistently near unity, agreeing with ω(w') that these are higher frequency (near-N) waves characteristic of mountain-generation.

PRELIMINARY CONCLUSIONS

w' data can be extracted from the balloon ascent rate to improve sonde gravity wave analysis. w' picks out near-N waves characteristic of orographic wave environments unlike Stokes analysis, which typically identifies near-f waves.

w' measurements are in broad agreement with WRF model comparisons, aircraft data comparisons, and spectral overlap with T' and u', though a more comprehensive analysis is needed to validate the technique.

w'-based analysis suggests that the wave packets observed on 19 June with the same T', u', v', and w' vertical wavelengths correspond to near-N waves having $E_K/E_P \approx 1$, with T' measurements potentially susceptible to non-wave sources of corruption. Stokes parameter analysis of the same dataset identifies primarily near-inertial waves, indicating the complementary benefits of using the two techniques.

Sonde trajectory data provides an excellent utility for mapping sonde-derived wave parameters in three dimensions, highlighting the inclined nature of sonde ascent profiles and actual vertical wavelengths larger than those obtained by assuming the profiles are vertical. Wave parameter calculations will ultimately benefit from adjustments accounting for such inclined ascent profiles.

ACKNOWLEDGMENTS

DEEPWAVE is funded by the National Science Foundation (NSF), the Office of Naval Research (ONR), and the Naval Research Laboratory (NRL). Radiosonde data were provided by the National Center for Atmospheric Research (NCAR) and the German Aerospace Center (DLR). Model forecasts were provided by DLR, with WRF simulations run by Johannes Wagner.

REFERENCES

Eckermann, S. D. (1996). Hodographic analysis of gravity waves: Relationships among Stokes parameters, rotary spectra and cross-spectral methods. J. Geophys. Res.Atmos., 101(D14), 19169-19174.

Kantha, L.H., et al. (2015). Retrieval of gravity wave properties in the lower atmosphere from radiosondes. Manuscript being submitted for publication.

Murphy, D.J., et al. (2014). Radiosonde observations of gravity waves in the lower stratosphere over Davis, Antarctica. J. Geophys. Res. Atmos., 119, 11,973-11,996, doi:10.1002/2014JD022448.

Zhang, S. D., et al. (2012). High vertical resolution analyses of gravity waves and turbulence at a midlatitude station. J. Geophys. Res. Atmos., 117, D02103, doi:10.1029/2011JD016587.